

# MACHINE LEARNING FOR THE LANL ELECTROMAGNETIC ISOTOPE SEPARATOR

A. Scheinker\*, K. Dudeck, C. Leibman  
 Los Alamos National Laboratory, Los Alamos, NM 87544, USA.

## Abstract

The Los Alamos National Laboratory electromagnetic isotope separator (EMIS) utilizes a Freeman ion source to generate beams of various elements which are accelerated to 40 keV and passed through a 75-degree bend using a large dipole magnet with a radius of 1.2 m. The isotope mass differences translate directly to a spread in momentum,  $\Delta p$ , relative to the design momentum  $p_0$ . Momentum spread is converted to spread in the horizontal arrival location  $\Delta x$  at a target chamber by the dispersion of the dipole magnet  $\Delta x = D(s)\Delta p/p_0$ . By placing a thin slit leading to a collection chamber at a location  $x_c$  specific isotope mass is isolated by adjusting the dipole magnet strength or the beam energy. The arriving beam current at  $x_c$  is associated with average isotope atomic mass, giving an isotope mass spectrum  $I(m)$  measured in mA. Although the EMIS is a compact system (5 m) setting up and automatically running at an optimal isotope separation profile  $I(m)$  profile is challenging due to time-variation of the complex source as well as un-modeled disturbances. We present preliminary results of developing adaptive machine learning-based tools for the EMIS beam and for the accelerator components.

## INTRODUCTION

The Los Alamos National Laboratory electromagnetic isotope separator (EMIS) utilizes a Freeman ion source to generate beams of various elements [1, 2], which are then accelerated to  $\sim 40$  keV and passed through a 75-degree bend using a large dipole magnet with a radius of 1.2 m [3]. Because the isotopes are accelerated to a common kinetic energy their mass differences translate directly to a spread in momentum,  $\Delta p$ , relative to the design momentum  $p_0$ . Momentum spread is then converted to a change in the horizontal arrival location  $\Delta x$  at a target chamber through the dispersion of the dipole magnet:  $\Delta x = D(s)\Delta p/p_0$ .

By placing a thin slit leading to a collection chamber at a location  $x = x_c$  it is possible to isolate specific isotope mass by sweeping the dipole magnet strength or the beam energy. The arriving beam current at  $x_c$  can be associated with average isotope atomic mass, resulting in an isotope mass spectrum  $I(m)$  measured in mA, as shown in Fig. 1 for a well-tuned EMIS with good isotope separation. Although the EMIS is a compact system (5 m) setting up and running at an optimal configuration at which the cleanest isotope separation is achieved with a desired  $I(m)$  profile can be challenge due to time-variation of the complex source as well as un-modeled disturbances. In this work we present

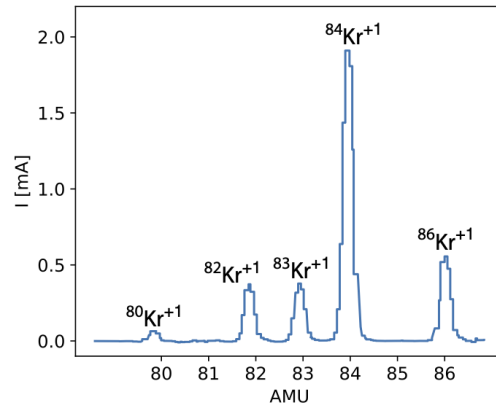


Figure 1: A typical Krypton spectrum is shown for a well tuned EMIS setup with sharp peaks between isotopes.

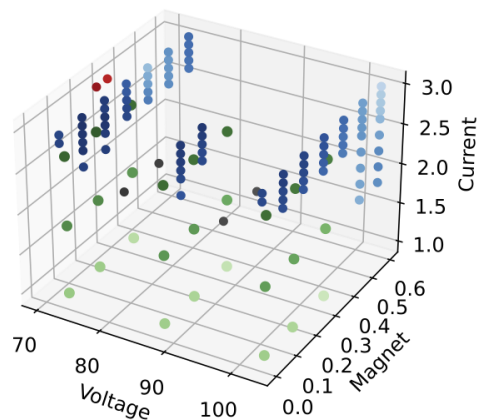


Figure 2: Data points collected for initial ML studies.

preliminary results of developing machine learning-based tools for the EMIS beam and for the accelerator components.

Initial data collection was carried out by adjusting the source voltage, the current of the source filament, and the current of a source magnet. For each setting the dipole magnet strength was swept over a wide range in order to record a full isotope spectrum  $I(m)$ . Figure 2 shows the data points which were collected during preliminary studies, with different colors corresponding to different collection days and different shades corresponding to the peak collector current at AMU 84.

## ML MODELS

We first demonstrated a neural network (NN) design which acts as a surrogate model,  $F(\mathbf{c})$ , mapping the set of controlled or measured EMIS parameters  $\mathbf{c} = (c_1, c_2, c_3)$ , which

\* ascheink@lanl.gov

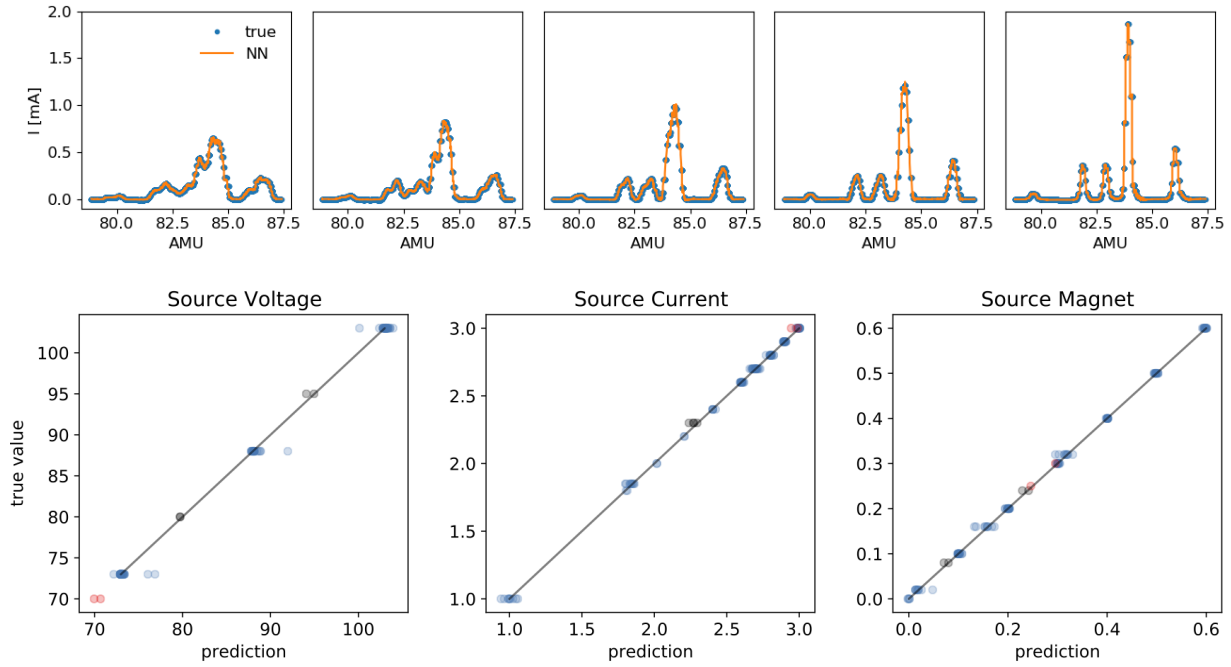


Figure 3: Top: Examples of generated spectra  $I(m)$  based on the trained NN. Bottom: Inverse function approximating NN for mapping a measured spectrum  $I(m)$  back to the three source parameters.

were the source current, voltage and source magnet current, to an estimate of the mass spectrum

$$F : \mathbf{c} \rightarrow \hat{I}(m), \quad (1)$$

by utilizing a supervised learning approach which minimized a cost based on the  $L^2$  difference between the predicted and measured spectra:

$$C = \int |I(m) - \hat{I}(m)|^2 dm. \quad (2)$$

Examples of the close match between predicted and measured spectra are shown in Fig. 3.

A second approach was to utilize a neural network as an inverse model  $F^{-1}(I(m))$  which enables the use of a measured spectrum  $I(m)$  as a diagnostic of various EMIS parameters via the inverse map

$$F^{-1} : I(m) \rightarrow \hat{\mathbf{c}}, \quad (3)$$

where the cost being minimized was now the mean squared error between predicted and set EMIS parameters:

$$C = \frac{1}{3} \sum_{i=1}^3 (c_i - \hat{c}_i)^2. \quad (4)$$

The accuracy of the inverse mapping is shown in Fig. 3.

## APPLICATIONS

The forward model can be used for EMIS optimization by quickly scanning over a large parameter space to map

parameter settings to an optimal mass spectrum  $I(m)$  with the cleanest isotope separation.

The inverse map has the potential to track time-varying parameter values  $\mathbf{c}(t)$  by continuously mapping a time varying spectrum  $F^{-1} : I(m,t) \rightarrow \hat{\mathbf{c}}(t)$ .

We these NN models can be used together with adaptive feedback control algorithms to develop adaptive machine learning (AML) tools that are robust to the time-varying nature of the EMIS source to serve as adaptive controls and adaptive virtual diagnostics for the EMIS system.

For adaptive tuning we utilize a recently developed form of adaptive feedback control which is designed for the stabilization and optimization of analytically unknown nonlinear time-varying systems of the form

$$\dot{\mathbf{x}} = \mathbf{f}(\mathbf{x}, \mathbf{c}, t), \quad (5)$$

$$C(\mathbf{x}, \mathbf{c}, t) = y(\mathbf{x}, \mathbf{c}, t) + n(t), \quad (6)$$

where  $\mathbf{x}(t)$  are physical parameters of interest such as, for example, the  $I(m)$  spectrum and the  $\mathbf{c}$  are controlled parameters,  $y(\mathbf{x}, \mathbf{c}, t)$  is a measurable analytically unknown output function such as the maximum value of the 84 AMU peak of  $I(m)$ , and  $n(t)$  is random noise [4, 5]. This adaptive tuning method has been utilized for complex time-varying problems such as the real-time control of the  $(z, E)$  longitudinal phase space of intense electron beams in the LCLS free electron laser at SLAC National Accelerator Laboratory [6].

The ES algorithm tunes parameters according to

$$\frac{dc_i}{dt} = \sqrt{\alpha\omega_i} \cos(\omega_i t + kc), \quad (7)$$

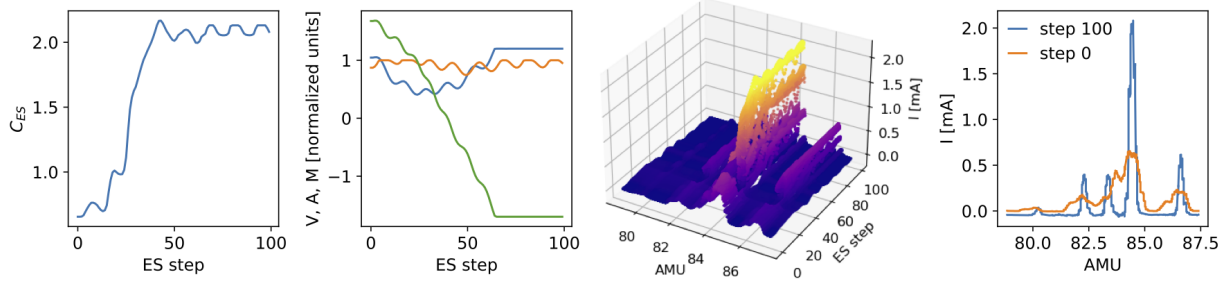


Figure 4: Adaptive tuning of input parameters for maximization of  $I(m)$  peak current showing evolution of normalized  $V, A, M$  parameter values, evolution of the  $I(m)$  spectrum, and the initial and final spectra.

where  $\alpha$  and  $\omega_i$  control the size of the dithering amplitudes,  $k$  is a feedback gain, and the  $\omega_i$  are distinct dithering frequencies. Note that  $C$  is a noise-corrupted measurement of the analytically unknown function  $y$ . For large  $\omega_i$ , using controller, Eq. (7) results in average parameter dynamics

$$\frac{d\bar{\mathbf{c}}}{dt} = -\frac{k\alpha}{2} \nabla_{\bar{\mathbf{c}}} C. \quad (8)$$

Here we define our cost function as  $C = \max_m \{I(m)\}$ , and take the following approach.

**Step 1:** Utilize a quick parameter scan, as shown in Fig. 2 to learn a neural network-based mapping  $F: \mathbf{c} \rightarrow \hat{I}(m)$ .

**Step 2:** Perform an extremely fast (ms per iteration by utilizing the NN) constrained digital iterative optimization based on a finite difference approximation of Eq. (7) of the form

$$\begin{aligned} c_i(n+1) &= c_i(n) + \Delta_t \sqrt{\alpha \omega_i} \cos(\omega_i n \Delta_t + kC(n)), \\ \hat{I}(m, n+1) &= F(\mathbf{c}(n+1)), \\ C(n+1) &= \max_m \{\hat{I}(m, n+1)\}. \end{aligned}$$

We demonstrate such an approach by starting with bad settings for  $V, A, M$ , which results in the poorly separated spectrum shown at step 0 in Fig. 4. The source parameters  $V, A, M$  are then adaptively tuned within constraints of the span of the training data that was collected as shown in Fig. 2 in order to automatically maximize the cost function  $C$ . The results of the tuning algorithm are shown in Fig. 4 with convergence to the maximum within  $\sim 40$  steps and a 3D view of the path the parameters take during optimization is shown in Fig. 5.

## CONCLUSIONS

We have demonstrated preliminary results on the benefit of simple adaptive ML for automatic optimization and tuning of an electromagnetic isotope separator. Our next steps are to update the digital data acquisition system of the Los Alamos EMIS in order to collect large data sets and develop sophisticated AML-based controllers and diagnostics.

## ACKNOWLEDGEMENTS

Work funded by Los Alamos National Laboratory.

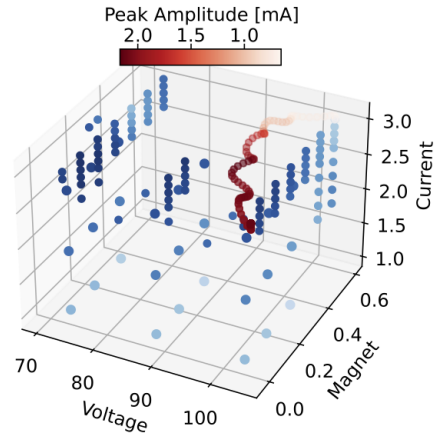


Figure 5: Adaptive convergence (red) in 3D parameter space relative to NN model training points (blue).

## REFERENCES

- [1] D. J. Chivers, “Freeman ion source: An overview (invited),” *Rev. Sci. Instrum.*, vol. 63, no. 4, pp. 2501–2506, 1992. doi:10.1063/1.1142874
- [2] J. Freeman, “A new ion source for electromagnetic isotope separators,” *Nucl. Instrum. Methods*, vol. 22, pp. 306–316, 1963. doi:10.1016/0029-554X(63)90257-X
- [3] I. N. Draganic, C. P. Leibman, L. J. Rybarczyk, T. M. Bronson, and K. W. Dudeck, “Hot filament performance in a freeman ion source,” *1*, vol. 2011, 2018, p. 030 005. doi:10.1063/1.5053266
- [4] A. Scheinker and M. Krstić, “Minimum-seeking for clfs: Universal semiglobally stabilizing feedback under unknown control directions,” *IEEE Trans. Autom. Control*, vol. 58, no. 5, pp. 1107–1122, 2013. doi:10.1109/TAC.2012.2225514
- [5] A. Scheinker and D. Scheinker, “Bounded extremum seeking with discontinuous dithers,” *Automatica*, vol. 69, pp. 250–257, 2016. doi:10.1016/j.automatica.2016.02.023
- [6] A. Scheinker, A. Edelen, D. Bohler, C. Emma, and A. Lutman, “Demonstration of model-independent control of the longitudinal phase space of electron beams in the linac-coherent light source with femtosecond resolution,” *Phys. Rev. Lett.*, vol. 121, no. 4, p. 044 801, 2018. doi:10.1103/PhysRevLett.121.044801